Physical Aging of Polycarbonate: Elastic Modulus, Hardness, Creep, Endothermic Peak, Molecular Weight Distribution, and Infrared Data

Victor A. Soloukhin,*,† José C. M. Brokken-Zijp,† Otto L. J. van Asselen,‡ and Gijsbertus de With†

Laboratory of Solid State and Materials Chemistry, Eindhoven University of Technology, P.O. Box 513, 5600 MB Eindhoven, The Netherlands, and Laboratory of Polymer Technology, Eindhoven University of Technology, P.O. Box 513, 5600 MB Eindhoven, The Netherlands

Received March 10, 2003; Revised Manuscript Received July 23, 2003

ABSTRACT: For the first time, load and depth sensing indentation (DSI) was used in order to monitor physical aging of bisphenol A polycarbonate for 30 months at room temperature and for 1 month at an elevated temperature. The DSI experiments were combined with differential scanning calorimetry, gel permeation chromatography, and infrared spectroscopy. The endothermic peak of polycarbonate shifted toward higher temperatures upon aging at an elevated temperature and did not change its location upon aging at room temperature. The elastic modulus and hardness of polycarbonate increased in a stepwise fashion during aging at room temperature. The molecular weight distribution broadened slightly, and the trans−trans conformational population increased during annealing. No simple correlation between changes in the mechanical properties and the shift of the endothermic peak during annealing was found. These changes seem to be caused by phenomena of different nature; namely, the changes in the mechanical properties appeared to have a reasonable correlation with free volume relaxation of the polymer, whereas the changes in the endothermic peak may be associated with internal energy changes. The similarities and differences between our results and the results of others are discussed.

1. Introduction

Presently, polycarbonate of bisphenol A (4,4′-isopropylidenediphenol) is an engineering material of major importance. Its good optical transparency and superb toughness have promoted it for a variety of industrial applications.[1,2] Over time, however, properties of polycarbonate change, causing, for example, embrittlement, or in other words the polycarbonate ages. Though these changes are typically minor, they still can be undesirable for a plastic part intended for long-term use, particularly, when failure of the part can be a result of these changes.[3,4] It is generally believed that these changes are related to the structural modifications occurring upon aging. As polycarbonate, or any other glassy polymer, is cooled below its glass transition temperature, molecular mobility decreases significantly, and the molecules are unable to reach an equilibrium packing density and conformational structure with respect to temperature.[5] The process of relaxation toward equilibrium is commonly referred to as physical aging. It can occur at an elevated temperature, e.g., during an experimentally carried out annealing process,[5,6] as well as at room temperature.[7]

The phenomena taking place in polycarbonate upon physical aging have been observed by means of a large number of analytical techniques such as tensile and creep measurements,[6,8,9] dynamic mechanical thermal analysis (DMTA),[3,10−13] differential scanning calorimetry (DSC),[6,14−17] positron annihilation lifetime spectroscopy (PALS),[5,9,18] Doppler broadening spectroscopy (DBS),[18] dilatometry,[3,8,15,19] Fourier transform infrared spectroscopy (FTIR),[7,12,20−24] Raman difference spectroscopy (RDS),[20] and solid-state nuclear magnetic resonance spectroscopy (NMR).[3] Although significant scientific knowledge has been gathered on the matter, the precise physical origin of physical aging phenomena is not fully understood. One of the remaining questions is the reason for occurrence of the enthalpy and volume relaxation changes in different time frames with respect to aging of polycarbonate at different temperatures.

In the meantime, a new analytical technique capable of providing information for elastic, plastic, and creep properties of materials has emerged, known as nanoindentation.[25] Also referred to as load and depth sensing indentation (DSI), this technique has proven itself as a powerful tool to characterize the above-mentioned mechanical properties and has been broadly used for inorganic substances for over a decade. On the contrary, for polymeric substances this technique has been limitedly applied. It will be shown in this paper that DSI can be used to accurately estimate the elastic modulus, hardness, and creep behavior of polycarbonate and even to observe subtle changes occurring in these properties upon physical aging.

In the present work we examine physical aging of polycarbonate by means of DSI, DSC, gel permeation chromatography (GPC), attenuated total reflection infrared (ATR-IR), and FTIR transmission spectroscopes in combination. The information obtained is compared with literature data. The results indicate a possible cause for different findings after volumetric and enthalpy relaxation experiments.

2. Experimental Section

2.1. Material and Specimens. Polycarbonate of bisphenol A used in this work was a commercially available optically transparent Lexan 9030 sheet (G.E. Plastics, Bergen op Zoom, The Netherlands) with an average molecular weight of approximately 30 000 according to PS standards. The chemical structure of polycarbonate of bisphenol A is given in Figure 1.

† Laboratory of Solid State and Materials Chemistry.
‡ Laboratory of Polymer Technology.
* Corresponding author: e-mail V.A.Soloukhin@tue.nl; Fax +31 40 2445619; Tel +31 40 2473053.

10.1021/ma0342980 CCC: $25.00
Published on Web 08/30/2003

Table 1. Specimens Used for the Physical Aging Experiments[a]

	specimens	t_{rt} (days)	T_{rt} (°C)	t_{rej} (h)	T_{rej} (°C)	t_{an} (h)	T_{an} (°C)	analytical techniques
set A	A1	0	22 ± 3					DSI
	A2	40	22 ± 3					DSI
	A3	160	22 ± 3					DSI
	A4	230	22 ± 3					DSI
	A5	255	22 ± 3					DSI
	A6	525	22 ± 3					DSC
	A7	720	22 ± 3					DSI
	A8	900	22 ± 3					DSI, DSC
	A9	950	22 ± 3					DSI, FTIR,[c] GPC
set B	B1	870	22 ± 3	1	160 ± 2	0	125 ± 5	DSI, DSC, ATR-IR, FTIR,[c] GPC
	B2	870	22 ± 3	1	160 ± 2	16	125 ± 5	DSI, DSC, ATR-IR, GPC
	B3	870	22 ± 3	1	160 ± 2	24	125 ± 5	DSI, DSC, ATR-IR, GPC
	B4	870	22 ± 3	1	160 ± 2	72	125 ± 5	DSI, DSC, ATR-IR, GPC
	B5	870	22 ± 3	1	160 ± 2	168	125 ± 5	DSI, DSC, ATR-IR, GPC
	B6	870	22 ± 3	1	160 ± 2	336	125 ± 5	DSI, DSC, ATR-IR, FTIR,[c] GPC
	B7	870	22 ± 3	1	160 ± 2	672	125 ± 5	DSI, DSC, ATR-IR, FTIR,[c] GPC
set C	C1	300	22 ± 3			336	80 ± 5	DSI
	C2	935[b]	22 ± 3			336	80 ± 5	DSI

[a] Set A consists of specimens aged at room temperature for different periods of time t_{rt} at temperature T_{rt}, set B consists of specimens rejuvenated at 160 ± 2 °C for 1 h and annealed for different periods of time t_{an} at temperature T_{an} equal to 125 ± 5 °C, and set C consists of specimens annealed for 336 h at T_{an} equal to 80 ± 5 °C. Additionally, the analytical techniques used for each specimen are included. [b] Specimen was aged at room temperature for 300 days at 22 ± 3 °C, annealed for 336 h at 80 ± 5 °C, and then aged at T_{rt} again for 635 days. [c] FTIR stands for Fourier transform infrared transmission measurements.

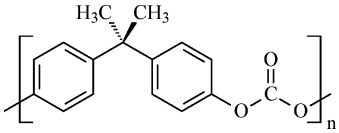

Figure 1. Chemical structure of polycarbonate of bisphenol A.

The extruded polycarbonate, which is not UV protected and without Mar resistant surface treatment, has an elastic modulus (E) of 2.35 GPa (ISO 527 for 1 mm/min) and a Vicat softening temperature of 145 °C (ISO 306), as quoted by the manufacturer. The polycarbonate was purchased as 100 cm^2 and 0.2 cm thick rectangular plates. Three plates of the same batch were kept at ambient atmosphere (T = 22 ± 3 °C and relative humidity of 75 ± 10%) in the dark and used as source material for three sets of specimens. Set A was aged at room temperature, while sets B and C were aged at elevated temperatures (Table 1). Rectangular specimens of approximately 1 × 1 cm^2 in size were sawn out of the plates at the chosen periods of time and then subjected to thermal treatment, ATR-IR, FTIR transmission, DSC and GPC analyses, and load and depth sensing indentation experiments.

For aging experiments at room temperature, the specimens were tested by means of DSI after an aging time (t_{rt}) of 0, 40, 160, 230, 255, 720, 900, and 950 days, respectively (specimens A1−A5 and A7−A9 in Table 1). Since the exact time of the extrusion of the plate was not known and, moreover, it is believed that the lifetime of the plate was less than 1 month, the first specimen tested (A1) is considered as the starting point (t_{rt} = 0 days) for the all following specimens in the present work. Specimen A9 was subjected additionally to FTIR transmission and GPC experiments.

For sub-T_g isothermal annealing experiments, further mentioned shortly as annealing experiments, the specimens were machined out of the second plate aged for 870 days. The specimens placed separately from each other in a closed glass Petri dish (11 cm in diameter) were located in an air-circulated heating chamber with a temperature of 160 ± 2 °C for rejuvenation. The rejuvenation process lasted for 1 h, and within a minute thereafter, the specimens were quenched by an air blow. Specimen B1 was withdrawn out of the heating chamber and air-cooled to room temperature, when a temperature of 125 °C was reached. The rest of set B (specimens B2−B7 in Table 1) was kept in the heating chamber for the chosen periods of time (t_{an}) for annealing at 125 ± 5 °C, which is approximately 20 °C below the nominal T_g. Once a specimen was taken out of the heating chamber, it was subjected for ATR-IR, DSC, and DSI analyses within 24 h, and a month later three specimens (B1, B6, and B7 in Table 1) were subjected to additional FTIR transmission measurements. Two months after the annealing experiments, every specimen of this set was subjected to a GPC analysis. To avoid any uncertainties of whether 2 months of postaging altered the molecular weight distribution (MWD) of the specimens, an additional specimen was rejuvenated and immediately subjected for GPC analysis. The result for this specimen perfectly matched the MWD obtained for specimen B1 and showed thus no changes in the MWD of the specimens during 2 months of postaging.

Furthermore, prior to DSI experiments on specimen C1, this specimen was aged at room temperature for 300 days and then annealed in an air-circulated heating chamber for 336 h at 80 ± 5 °C (see Table 1). The DSI measurements on specimen C1 were performed within a week after annealing. Specimen C2 was aged at room temperature for another 635 days after aging steps similar to those of specimen C1.

2.2. Load and Depth Sensing Indentation. a. Apparatus. Load and depth sensing indentations were carried out at room temperature and ambient atmosphere using a home-built apparatus, a schematic illustration of which is shown in Figure 2. The apparatus is equipped with a Berkovich-type diamond indenter, i.e., a three-sided pyramid with the inclination angle of 65.3° between the faces and the loading axis.[26] The device permits up to 25 indentations to be made in one run at loads ranging from 1 to 1000 mN with a range of possible rates from 0.4 to 20 nm/s. This apparatus allows experiments to be performed only under displacement control and has the maximum displacement of 30 μm.

The calibration procedure suggested by Oliver and Pharr[25] was implemented to correct for the load frame compliance of the apparatus and the imperfect shape of the indenter tip. The area function of this indenter was calibrated using B270 glass (Schott, Jena, Germany), whose elastic modulus was determined independently as 75 ± 1 GPa using the pulse-echo method. The compliance of this system as determined from the unloading curve was 0.3 nm/mN, and the projected area of the indenter (A) was related to the contact depth (h_c) of the indentation by $A = ah_c^2 + bh_c$ (a = 24.5 and b = 5.71 μm), being equivalent to a tip radius of approximately 0.9 μm. The calibration was performed using B270 glass for a depth range of 0.1−2.9 μm, where the maximum indentation depth was restricted by the load limitation.[27]

For better understanding of the indentation process a brief description follows. To make an indentation, a holder clamped in the apparatus with a specimen located upon it has to be

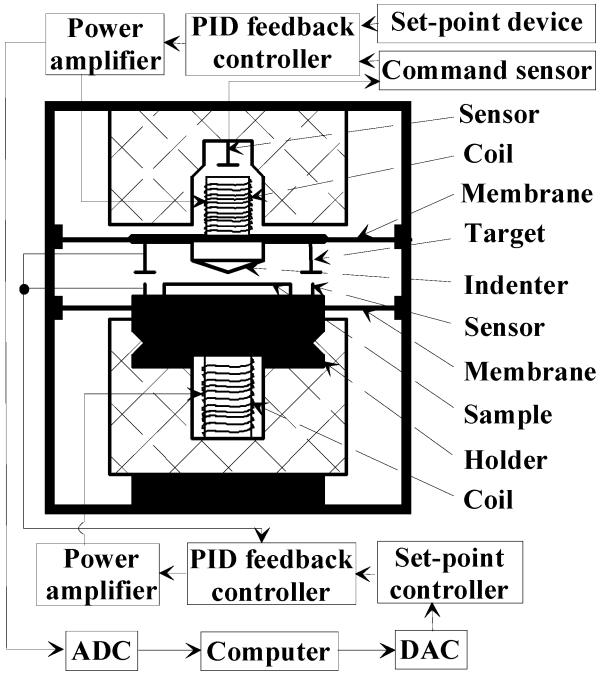

Figure 2. A schematic figure of the load and depth sensing indentation apparatus.

adjusted manually to the vicinity of the indenter. To comply with the possibility of the surface search, it is required to make this adjustment in such a way that the surface of the specimen is situated less than 300 μm from the indenter tip. After that, the surface of the specimen is found in an automatic mode, and the loading process starts. After receiving a signal from a set-point controller, a *lower* power amplifier supplies voltage to a *lower* coil via a *lower* proportional-integral-derivative (PID) feedback controller (Figure 2). This causes an upward movement of the specimen together with the indenter having the smallest step of 0.5 nm. This movement induces a response in a command sensor of the indenter, indicating that the indenter moved from the position fixed by a set-point device. The signal coming from the command sensor causes an increased voltage in an *upper* coil supplied by an *upper* power amplifier via an *upper* PID feedback controller to compensate for the movement and to return the indenter at the originally fixed position. The above-mentioned process repeats until the voltage in the *upper* coil is proportional to a requested maximal indentation load (P_{max}) corresponding to a force $F = IlB$, where l is the length of a coil, I is the current in a coil, and B is the magnetic field (Figure 3a,b). Thereafter, either an unloading or a holding process (Figure 3d) starts, which proceeds in a way similar to the loading process. The apparatus is equipped with three target-displacement sensors (note that only two of them are shown in Figure 2) to measure the displacement occurring during the indentation and to ensure horizontal positioning of the holder. A computer collects the indentation information converted via an analog-to-digital converter (ADC) and allows interfering with the system via a digital-to-analog converter (DAC). The apparatus also provides the possibility to move the holder in horizontal directions in a well-controlled fashion.

b. Elastic Modulus and Hardness Calculations. As was proposed by Oliver and Pharr,[25] elastic modulus and hardness can be determined from indentation data obtained during one complete cycle of loading and unloading. The effective elastic modulus can be calculated using the equation $E_{eff} = (1/\beta)\cdot(\sqrt{\pi}/2)(S/\sqrt{A})$, where S is the experimentally measured unloading stiffness (Figure 3a) and β is a geometrical constant equal to 1.034 for a Berkovich indenter.[28] The effective elastic modulus, due to elastic deformation in both the specimen and the indenter, is related to the specimen elastic modulus by $E = (1 - \nu^2)/[1/E_{eff} - (1 - \nu_i^2)/E_i]$, where E and ν are elastic (Young's) modulus and Poisson's ratio for the specimen,

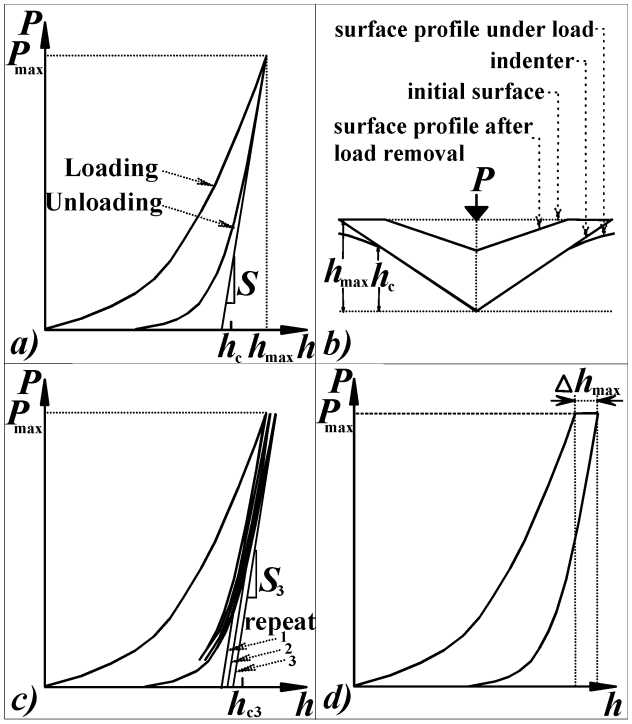

Figure 3. Schematic representation of load P vs indenter displacement h: (a) for one loading−unloading indentation circle, which is coupled with a schematic cross section of this process (b); (c) for three times repeated indentation at the same position; (d) for a creep experiment.

respectively, whereas E_i and ν_i are the same quantities, respectively, for the indenter. For diamond $E_i = 1141$ GPa and $\nu_i = 0.07$[29] were used. For polycarbonate $\nu = 0.4$[30] was used. It was assumed in the present work that the Poisson's ratio of polycarbonate is constant independent of aging temperature and time. Finally, the hardness H is defined by $H = P_{max}/A$.

The unloading stiffness, which is necessary for assessing the elastic modulus, was calculated after polynomial fitting of 90% of the unloading curve. Most of the elastic modulus and hardness data, presented in the present work, correspond to the second repeat (see the following section) of the indentation experiments. Indentation loads ranged from 4 to 1000 mN. Lower loads were dismissed as providing unreliable data due to relatively high surface roughness of the polycarbonate (see section 2.3).

Phenomena such as pile-up and sink-in, which may lead to some overestimate or underestimate of the contact area, respectively, and consequently to errors for the elastic moduli and hardness,[28,31] were not taken into account. As an example we show evidence of a small pile-up in Figure 4.

c. Repetitive Indentations with Different Loads. Repetitive indentations at the same position were done as follows. The indenter, once it reached a maximum load, is unloaded until 10% of P_{max}, and then the next indentation is set at the same position up to the same P_{max} with a maximum of 10 repeats. The indenter is totally unloaded after the last repeat. Then the holder with a specimen upon it is moved in a horizontal direction, and a new set of indentations, with another required load, is performed. The value of E and H was calculated for every unloading curve. A schematic representation of indentation, which consists of three repeats, is given in Figure 3c. The deliberate repetitive indentation measurements were performed on specimens A5 and C1 (Table 1).

d. Rate-Dependent Indentations. Rate-dependent indentations were performed on specimen A7 (Table 1) with rates (r) ranging from 0.5 to 20 nm/s, with three repeats at the same position and P_{max} equal to 10 mN. For the rest of the indentation experiments a rate of 10 nm/s (specimens A1−A5 and C1) or 15 nm/s (specimens A7−A9, B1−B7, and C2) was used.

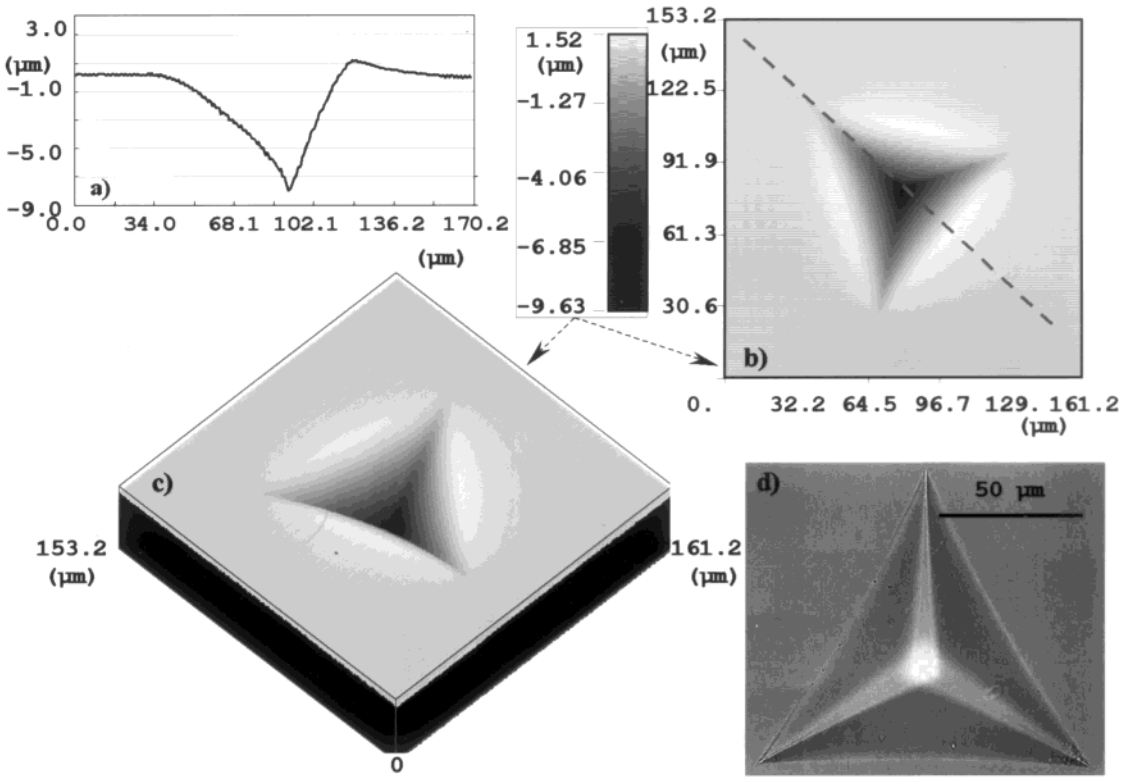

Figure 4. Confocal and optical data obtained for the indent after loading with 800 mN on specimen A8, namely, profile of the indent (a), 2-D confocal image of the indent (b), 3-D confocal image of the indent (c), and optical image of the indent (d). The profile (a) corresponds to the direction given in (b) as a dashed line.

e. Indentation Creep Measurements. Indentation creep measurements were performed as follows. The indenter, once it reached the maximum load, was kept under P_{max} for 10 min, and then the indenter was totally unloaded. Indentation creep measurements were performed with different loads, namely, 10, 50, 100, 500, and 1000 mN. The shift in the maximal penetration depth of the indenter (Δh_{max}), which occurred during the holding period, was used as a creep parameter. Only the annealed specimens forming set B (Table 1) were used for these measurements. A schematic representation of a typical indentation creep experiment is given in Figure 3d. For each particular load, the changes in the stresses occurred during the creep experiments were approximately constant for different annealing times. The estimated changes varied from 19.0 to 11.0% for the loads ranging from 10 to 1000 mN.

2.3. Optical and Confocal Microscopy. Optical microscopy was used for observation of the final indents, whereas confocal (NanoFocus μSurf confocal microscope) was used for profile measurements of the indents and roughness estimations. As an example, we show the optical (Figure 4d) as well as confocal (Figure 4b,c) micrographs of 800 mN load indent after a load and depth sensing indentation on specimen A8. The profile of the indent is shown in Figure 4a for the direction indicated with a dashed line in Figure 4b. The surface roughness of this specimen, as well as that of the others, was estimated being equal to $R_a = 0.45 \pm 0.05$ μm.

2.4. Enthalpy Relaxation Experiments. The enthalpy relaxation measurements were performed on the specimens (sets A and B in Table 1) using a Perkin-Elmer Pyris 1 differential scanning calorimeter. The calorimeter was calibrated using the fusion temperatures of gallium, indium, tin, lead, and zinc. The baseline was checked regularly over the period of experiments. All experiments were done in dry nitrogen with a flow rate of 20 mL/min.

Specimens A6 and A8, as representative for set A, were used for the enthalpy relaxation measurements. In the case of set B, all specimens were subjected to these experiments within 24 h once they were withdrawn from the heating chamber. Two to four samples were cut out of every specimen. These samples were weighed on a microbalance and sealed in standard 40 μL aluminum pans. The weight of the samples ranged from 4.0 to 8.0 mg.

For performing the DSC runs a heating rate of 10 K/min was chosen, which is generally used for physical aging experiments.[6,14,15] Initially, each sample was kept for 5 min at 60 °C for stabilization. This isothermal step was followed by thermal scans: heating to 170 °C and immediate cooling to 60 °C at 10 K/min. Subsequently, this process was repeated twice. Data obtained during the first heating scan were used to estimate the exact positioning of the endothermic peak, located in the T_g region, with respect to different aging temperatures and times. The second heating (or reheating) scan was used as a reference. The satisfactory superimposition of the second scans indicated that each sample attains a reproducible state with erased thermal history, once it was heated above T_g to 170 °C. The temperatures reflecting the shift of the endothermic peak are given in the Results section in terms of $T_{p,e}$ (extrapolated onset temperature), $T_{p,1/2}$ (half-step temperature), and $T_{p,max}$ (temperature at the maximum of the endothermic peak). The first two temperatures were assessed in a way similar to usual T_g estimations.[32]

2.5. GPC Analyses. The GPC experiments were carried out using a Waters model 510 pump, model 486 UV detector (at 254 nm), and model 410 refractive index detector (at 40 °C). Injections were done by a Waters model WISP 712 autoinjector with an injection volume of 50 μL. As a column set, a series consisting of a PLgel guard (5 μm particles), a 50 × 7.5 mm guard column, and two PLgel mixed-D (5 μm particles) 300 × 7.5 mm columns (40 °C) was used. Tetrahydrofuran (Biosolve, stabilized with BHT) was used as eluent at a flow rate of 1.0 mL/min. Data acquisition and processing were performed using Waters Millennium 32 (v 4.0) software. Calibration was done using PS standards with molecular weight from 580 to 7.1×10^6. Calculation of molecular weight distribution (MWD) of the polycarbonate specimens was performed using universal calibration with the Mark−Houwink parameters $a = 0.716$, $K = 0.000\ 114$ dL/g for polystyrene and $a = 0.67$, $K = 0.000\ 49$ dL/g for polycarbonate.

The solutions of the polycarbonate specimens were prepared as follows. Small samples of 5−6 mg, which were representa-

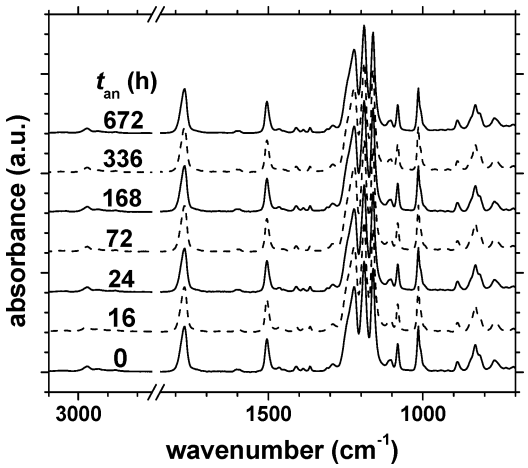

Figure 5. ATR-IR spectra obtained for the polycarbonate specimens depending on annealing time.

tive of the whole thickness of the polycarbonate plates, were separated from the chosen specimens. These samples were dissolved in 0.3 mL of dichloromethane and then diluted in 2.8−3.0 mL of tetrahydrofuran. The solutions were filtered through a 13 mm × 0.2 μm PTFE filter with polypropylene housing (Alltech, Deerfield, IL) prior to GPC analysis.

2.6. ATR-IR and FTIR Transmission Analyses. Attenuated total reflection infrared (ATR-IR) spectroscopy was used for further morphological analysis. Infrared spectra were recorded using an ATR slide-on accessory on the objective of a Biorad UMA 500 microscope coupled to a Biorad FTS 6000 FTIR spectrometer. The IR spectra were recorded with a resolution of 4 cm^{-1} co-adding 50 scans. A slide-on ATR crystal of germanium was used, permitting investigation of about 1 μm thick upper layers of the specimens. A typical area for collecting ATR-IR information was about 100 × 100 μm^2.

Since polycarbonate has a number of very strong infrared absorption bands, very thin slices had to be made from the specimens to be able to investigate these bands in transmission. Therefore, 1−1.5 μm thick slices were cut from the chosen polycarbonate specimens (specimens A9, B1, B6, and B7 in Table 1) by means of a Leica RM2165 microtome, equipped with a glass knife. The infrared spectra were recorded using the Biorad FTS 6000 FTIR spectrometer. Initially, spectra from each slice were recorded with a Biorad UMA 500 infrared microscope equipped with a mercury cadmium telluride (MCT) detector. The measured area was of about 30 × 30 μm. Spectra were recorded with a resolution of 2 cm^{-1} co-adding 100 scans. In the latter stage of the investigation the spectra were recorded from an area of 2 × 4 mm. In this case a deuterated triglycine sulfate (DTGS) detector was employed.

The IR spectra obtained for the source plates appeared to be identical to that known for amorphous polycarbonate of bisphenol A,[22] confirming thus a sufficient purity of the purchased polycarbonate. Typical IR spectra of polycarbonate obtained by means of ATR-IR spectroscopy after the annealing experiments are given in Figure 5.

The FTIR transmission data collected from the slice made of specimen A9 were compared with the FTIR transmission data collected from the same slice after it was rejuvenated. The rejuvenation process for this slice was done in the same way as that used prior to the annealing experiments of set B.

A number of infrared bands are sensitive to conformational changes in polycarbonate upon thermomechanical modifications.[7,20,22] Three bands described below were used to examine conformational changes in our specimens. The broad carbonyl band C=O has its maximum at approximately 1775 cm^{-1} and can be subdivided into contributions from trans−trans and trans−cis conformers at about 1767 and 1785 cm^{-1}, respectively. The skeletal vibration of the aromatic ring, the so-called C−C aromatic in-plane stretching, exhibits a doublet at approximately 1600 cm^{-1}, which can be separated into trans−trans and trans−cis conformational contributions at 1594 and 1604 cm^{-1}, respectively. The C−O−C antisymmetric vibration is associated with a doublet having its maximum at approximately 1235 cm^{-1} and consists of trans−trans and trans−cis conformational contributions at 1252 and 1223 cm^{-1}, respectively. Differently from the general assignment of the C−O−C antisymmetric vibration, Dybal et al.[24] indicated after their ab initio quantum mechanical calculations that the high-frequency component should be assigned to the trans−cis conformational structure. In our work we stick to the general assignment for the 1235 cm^{-1} IR region.

Since IR spectra corresponding to specimens with identical (thermal) history exhibited some minor differences for different regions analyzed, a number of spectra were collected for each specimen and the mean spectra were calculated. These mean spectra were used for comparisons. Prior to comparison, these spectra were adjusted using the band at approximately 1504 cm^{-1} as an internal standard. This band corresponding to aromatic ring stretching was chosen since no conformation changes have been reported for it in the literature.

Additionally, it should be indicated that the mechanical modification of the analyzed samples (1−1.5 μm thick slices) upon their preparation could possibly contribute to the conformational interchange. In our case, some minor differences between the mean spectra of specimens B1, B6, and B7 were found at approximately 1083 and 1015 cm^{-1}. In the literature these bands are indicated as stress sensitive.[7]

3. Results and Discussion

Over about a decade, material scientists have been investigating mechanical properties of a wide spectrum of materials by means of load and depth sensing indentation technique. Largely, their research was focused on inorganic substances, whereas a rather restricted number of works have being devoted to polymeric materials. To our knowledge, until now no thorough DSI experiments have been performed examining the mechanical properties of polycarbonate of bisphenol A. Since some changes in mechanical properties of polycarbonate can be expected for different experimental conditions, such as indentation load, rate, and a number of repeats, due to viscoelasticity of the polymer,[33] a series of indentation experiments were carried out in order to monitor such changes in the elastic modulus and hardness of polycarbonate. In the first sections, the results of these experiments are given. Thereafter, our data for the physical aging experiments on polycarbonate are presented and discussed.

3.1. Load and Depths Sensing Indentation on Polycarbonate. a. Repetitive Indentations with Different Loads. The results of the DSI experiments performed on specimen C1 in order to monitor changes in the elastic modulus and hardness of polycarbonate depending on repetition number of indentation are presented in Figures 6 and 7 for different loads. The values obtained after 10 repeats for the elastic modulus and hardness vs the indentation contact depth and depending on indentation loads used are given in parts a and b of Figure 6, respectively. The same values for both mechanical properties vs the repeat number for five chosen loads are plotted in parts a and b of Figure 7 for the measured elastic modulus and hardness values, respectively. As one can see, with an increase in the indentation load, the elastic modulus and hardness decrease roughly by 10 and 35%, respectively. Creep, a phenomenon well-known for polymers, can explain these decreases. Indeed, for performing an indentation with a higher load, a longer period of time is required. Thus, the longer indentation time provides a longer time for material to creep. The somewhat larger scatter in the E and H values in the case of the low loads (Figure 6)

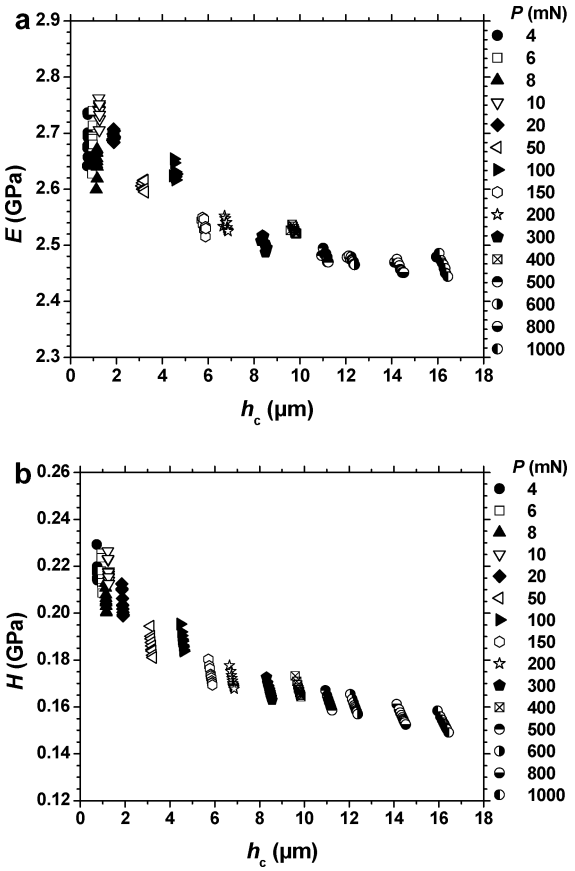

Figure 6. Elastic modulus (a) and hardness (b) vs the contact depth of the indenter after 10 repeats with every corresponding load on specimen C1.

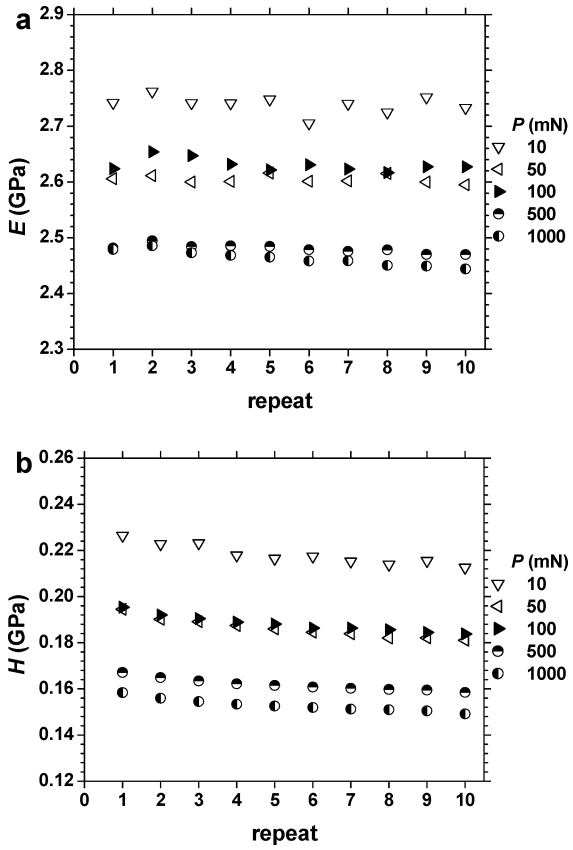

Figure 7. Elastic modulus (a) and hardness (b) vs the repeat number after indentations on specimen C1 with five different loads.

can be explained by surface roughness and less experimental precision in applying these loads. Moreover, as was indicated by Boersma et al.,[34] creep for freshly prepared polycarbonate is even more severe.

For each indentation load, a gradual small decrease in the hardness of polycarbonate can be clearly observed while indentations are repeated, as one can see from Figure 7b. This is obviously caused by an increasing indenter displacement upon repetitive indentation. The values of the elastic modulus appear to be independent of repetition, with an exception for the highest loads, where a slight decrease is observed (Figure 7a).

b. Rate Data. Rate-dependent indentation measurements were performed on specimen A7. The elastic modulus and hardness values measured vs the indentation rates used are given in parts a and b of Figure 8, respectively. As one can see, the elastic modulus is obviously less sensitive to changes in indentation rate than the hardness. Since a sample standard deviation of 10.3% for the elastic modulus values is comparable with the error of our DSI measurements, we conclude that within the experimental error the elastic modulus is independent of the indentation rate. For the hardness, on the other hand, an increase of almost 200% can be observed. The hardness data show that a rather drastic increase occurs between an indentation rate of 0.5 and 5 nm/s and that the hardness increase is small for further increase in rate.

Although for low indentation rates a clear rate dependence is observed, the dependence in the range 5−20 nm/s is limited. Therefore, for the indentation experiments on polycarbonate, a rate of 10 or 15 nm/s was used.

3.2. Physical Aging at Room Temperature. a. Elastic Modulus and Hardness. Load and depth sensing indentation experiments devoted to aging of polycarbonate at room temperature and ambient atmosphere were carried out over a period of $2^1/_2$ years. The elastic modulus and hardness vs the contact displacement, which corresponds to the indentation loads ranging from 4 to 1000 mN, are given in parts a and b of Figure 9, respectively.

A division of the E and H values in Figure 9 into two groups seems to be possible, with a major shift in the mechanical properties between the groups at approximately $t_{rt} = 160-230$ days. The scatter for the lower indentation loads, roughly below 100 mN or for $h_c < 4$ μm, appears to be somewhat larger than for the higher loads. This difference in scatter can be actually expected, since for the higher loads a requested load can be set with a higher precision than for the lower ones. Furthermore, in the case of the higher loads, the influence of the surface roughness can be neglected.

To make the separation into two groups more obvious, the values of hardness (loads above 90 mN) and the values of elastic modulus (independent of load) can be represented as E and H vs t_{rt} plots for a particular load. The data corresponding to the indentation load of 100 mN are shown in parts a and b of Figure 10 for the elastic modulus and hardness, respectively. In the case of elastic modulus of polycarbonate, an increase by 450 MPa, roughly from 2.20 to 2.65 GPa, can be observed (Figure 10a). On the other hand, for the hardness of polycarbonate (Figure 10b), an increase equal to ∼35 MPa can be observed. It is important to emphasize here that this stepwise change in the mechanical properties

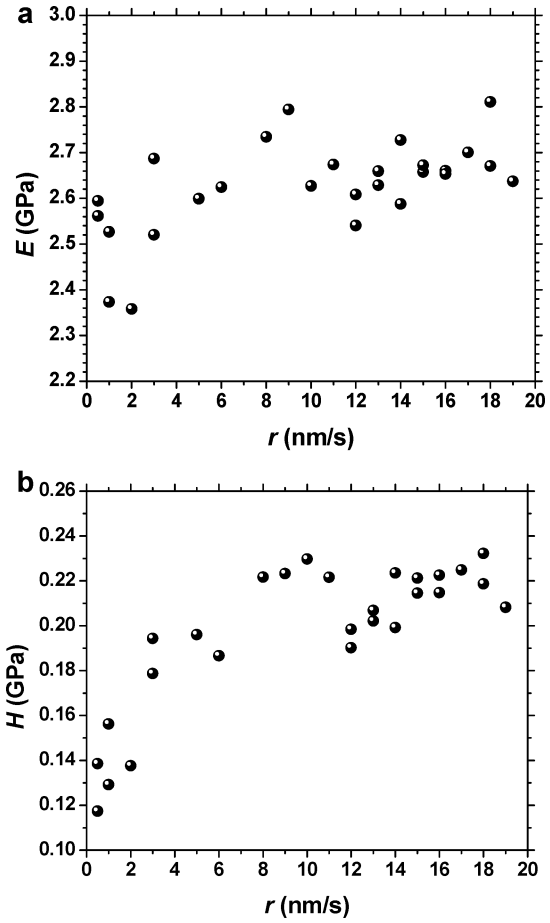

Figure 8. Elastic modulus (a) and hardness (b) vs the indentation rate corresponding to loading with 10 mN on specimen A7.

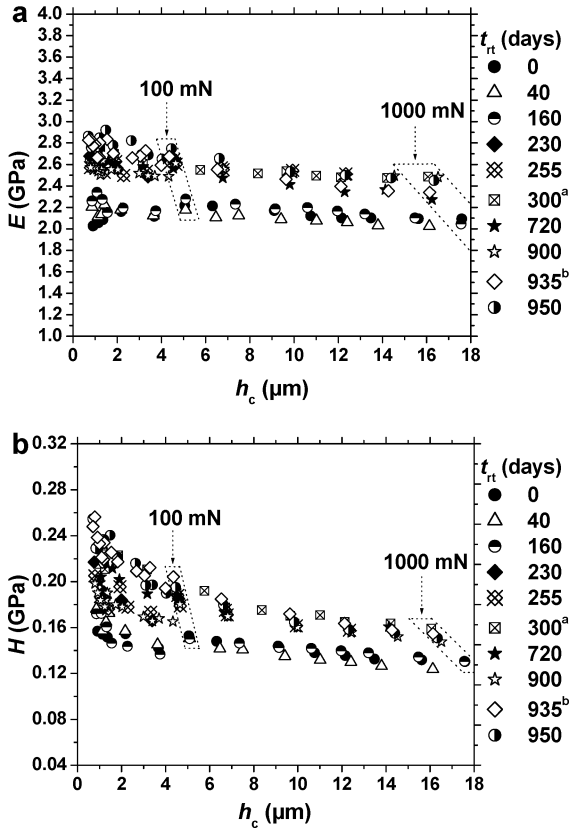

Figure 9. Elastic modulus (a) and hardness (b) vs the indentation contact depth corresponding to indentation with loads ranging from 4 to 1000 mN on the specimens with different aging time t_{rt}. The legends marked with superscripts a and b correspond to specimens C1 and C2, respectively.

occurred over a relatively short period of time, that is, 70 days, whereas before and after this change both mechanical properties appeared to be hardly dependent on time.

Additionally, the values for two specimens with a different thermal history, i.e., specimens C1 and C2, are incorporated in Figure 10. As one can see, no obvious differences in the elastic modulus and hardness for these two specimens as compared to specimens A4, A5, and A7−A9 can be observed. The overall picture suggests that, disregarding the aging time, the hardness is more sensitive to creep than the elastic modulus (Figure 9).

b. Enthalpy Relaxation Analysis. No obvious changes in the magnitude and location of the endothermic peak, in the glass transition step, were observed during the DSC runs on specimens A6 and A8. The values obtained, i.e., $T_{p,e} = 145.6 \pm 1.3$ and $T_{p,1/2} = 145.7 \pm 1.2$ °C, are in good agreement with the Vicat softening temperature of polycarbonate (145 °C), provided by the supplier, and in reasonable agreement with the $T_{p,e}$ and $T_{p,1/2}$ values that were measured for the rejuvenated polycarbonate (specimen B1 in Table 1). This observation is in line with a T_g stability of polycarbonate aged at room temperature indicated by Heymans.[7] No indication of crystallinity in the DSC scans for these specimens was found.

c. FTIR Transmission Analysis. From set A, only specimen A9 was examined with FTIR transmission spectrometry. The IR spectra were obtained from the slice made of this specimen before and after rejuvenation. A comparison between the mean spectra of A9 and "A9 rejuvenated" showed that the two bands of the three bands examined exhibited no changes in the conformational populations. A small difference was observed for the carbonyl band located at approximately 1775 cm^{-1}. This change, however, did not match an expected conformational trans-trans−trans-cis interchange pattern and was also not accompanied by similar changes in other IR regions. Hence, no clear evidence of conformational interchange during aging at room temperature was observed.

d. Discussion of Aging at Room Temperature. The experimental results highlighting the stepwise change in E and H of polycarbonate during aging at room temperature (Figures 9 and 10) appear to be rather peculiar, but they are not totally unexpected. Earlier, Wimberger-Friedl and de Bruin,[35] using the gradient column technique, showed an unusually sudden densification of polycarbonate. A sharp transition in volume recovery of polycarbonate happened after approximately 6 months of aging. Using dilatometry Robertson and Wilkes[15] reproduced this observation reporting a similar change in polycarbonate densification behavior after approximately 4 months of aging. A schematic representation of these two findings is given in Figure 11. Unfortunately, no well-established theory has been presented so far able to elucidate this peculiar transition in the densification behavior of polycarbonate. In our case, the observed stepwise increase in E and H occurred between approximately 5.3 and 7.6 months of aging and appeared thus to be in good agreement with

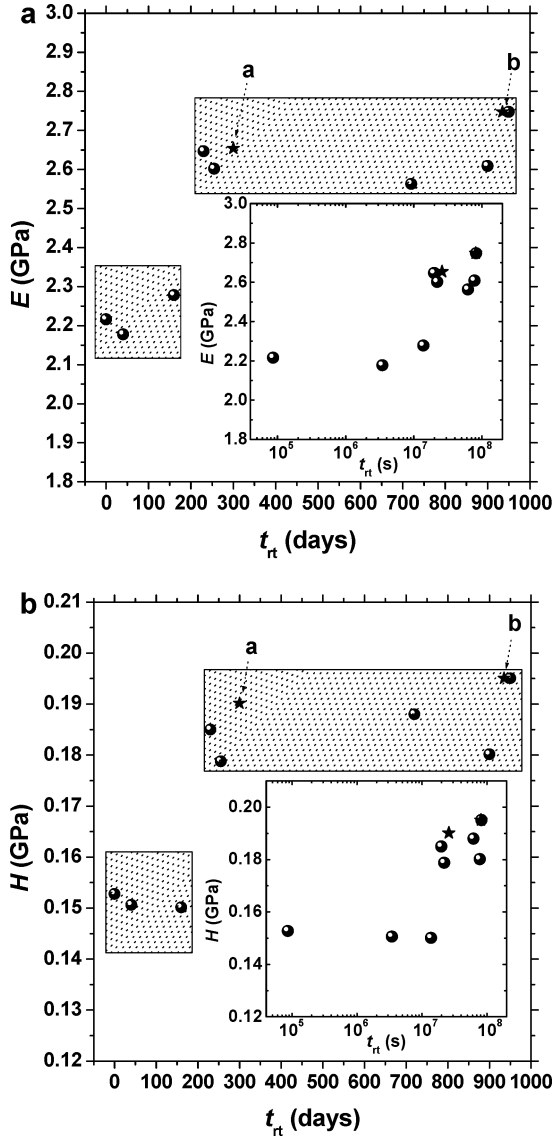

Figure 10. Elastic modulus (a) and hardness (b) vs the aging time t_{rt} obtained after indentation with 100 mN on the specimens forming set A. The stars in the plots marked by arrows with a and b correspond to specimens C1 and C2, respectively. The insertions are the same graphs in a logarithmic time scale.

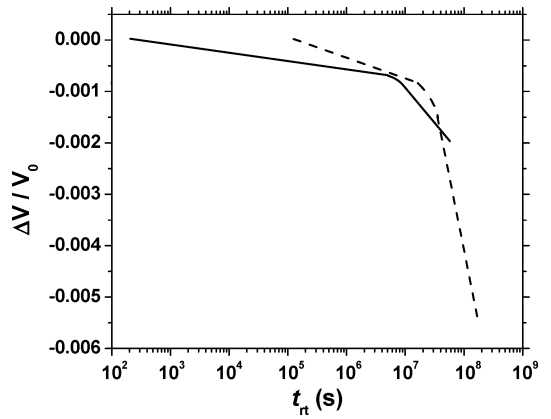

Figure 11. Schematic representations of volume recovery of polycarbonate at room temperature observed by Wimberger-Friedl and de Bruin[35] (dashed curve) and by Robertson and Wilkes[15] (solid curve).

work of Wimberger-Friedl and de Bruin. Upon further aging, no well-pronounced increase in the mechanical properties, which might be expected from Figure 11, was found, though.

Furthermore, the E values before (∼2.20 GPa) and after (∼2.65 GPa) the stepwise change (Figures 9a and 10a) appeared to also be in good agreement with DMTA results, which revealed changes in the storage modulus (E') depending on molecular orientation of polycarbonate at room temperature. Namely, Shelby et al.[3] showed that the storage modulus varied in a close to stepwise fashion once a minor molecular orientation in polycarbonate was established. The major shift from 2.10 to 2.60−2.85 GPa was observed when Herman's orientation function altered from 0 to just 0.033, whereas upon a further increase in orientation up to 0.170 only very minor changes in E' occurred. Unfortunately, Shelby et al.[3] provided no information concerning conformational changes in the molecular structure of polycarbonate.

3.3. Physical Aging at Elevated Temperature. a. Elastic Modulus and Hardness. The experimental information for annealing of polycarbonate at 125 °C over a period of 672 h was collected during the load and depth sensing indentation experiments with 10, 50, 100, 500, and 1000 mN on seven specimens (specimens B1−B7). The results corresponding to these measurements are shown in parts a and b of Figure 12 for the elastic modulus and hardness vs the annealing time, respectively. An initial comparison of the elastic modulus and hardness values for $t_{an} = 0$ to those for $t_{rt} = 0$ (Table 1) indicates that a 1 h rejuvenation period at 160 °C appeared to be insufficient for a full reverse of the preliminary aging at room temperature in terms of the mechanical properties investigated. Some changes occurring in the mechanical properties of polycarbonate during annealing could be observed, however. One can clearly see from Figure 12 that the elastic modulus and hardness increase with annealing time. Remarkably, the increase in the mechanical properties for "the upper layers" of polycarbonate (probed with $P = 10$ mN) appeared to be larger and more abrupt than for "the deeper layers" (see the dotted guide curves in Figure 12a,b). Furthermore, this trend repeats while moving layer by layer into the bulk up to ∼17 μm in depth, which corresponds to the highest loads used, i.e., 1000 mN. Note also that the most significant increase in the case of the low loads occurred during the first 24 h.

b. Creep Data. The results of the creep load and depth sensing indentation measurements on the annealed set (set B in Table 1) are given in Figures 13 and 14 for the shift in the maximum indentation depth vs the indentation load used and the annealing time, respectively. These results correspond to the indentation loads equal to those used for the elastic modulus and hardness evaluations, which were discussed above. One can see from Figure 13 that with the increase in indentation load the creep increases. How large the difference in creep due to annealing is appears to be obscure from Figure 13 for the indentation loads of 10, 50, and 100 mN. For the higher loads (500 and 1000 mN), the possibility of a subdivision into two parts can be noticed. The representation of the creep data as shifts occurring in the maximum indentation depth vs the annealing time makes the changes in creep due to annealing more obvious (Figure 14). Similar to the E and H vs t_{an} data for the low loads (Figure 12), a rather abrupt change for the creep values can be observed for the first 24 h, which is then followed by the step independent of further annealing. The independence of

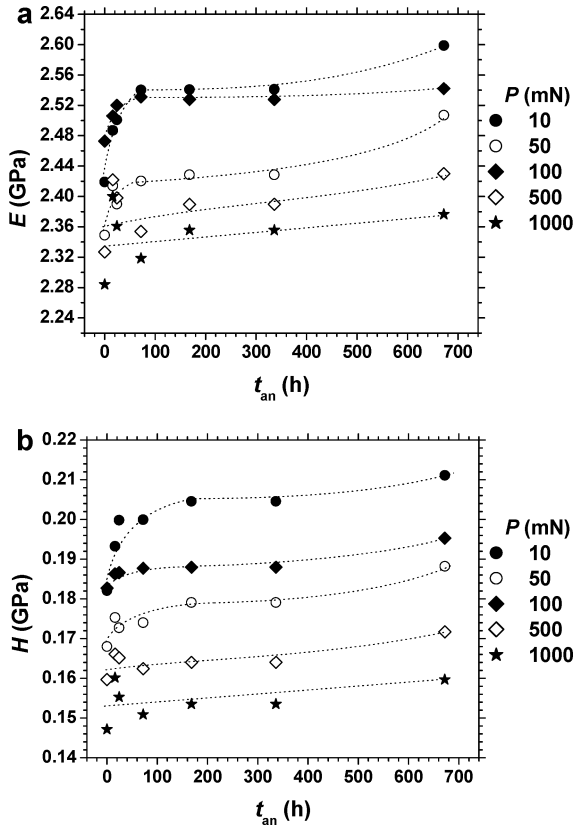

Figure 12. Elastic modulus (a) and hardness (b) vs the annealing time obtained after indentation on the specimens forming set B with 10, 50, 100, 500, and 1000 mN.

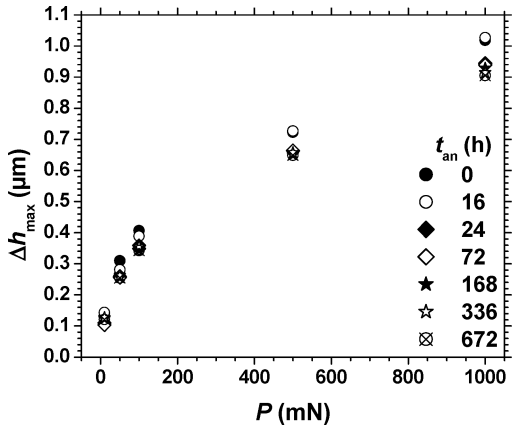

Figure 13. Shift in the maximum indentation depth vs the indentation load for the specimens with different annealing time.

creep for annealing longer than 24 h appears to be somewhat different compared to the trends observed for *E* and *H*, where a gradual growth takes place for the same specimens.

c. Enthalpy Relaxation Analysis. The experimental results obtained during the DSC measurements with specimens B1−B7 in order to monitor changes in the endothermic peak located in the T_g region of polycarbonate while annealing confirmed the earlier published results.[6,14,16] Indeed, the endothermic peak shifts toward higher temperatures and increases in magnitude with an increase in annealing time. In Figure 15 the measured $T_{p,e}$, $T_{p,1/2}$, and $T_{p,max}$ for specimens B1−B7 vs the annealing time are shown. No sign of crystallinity was found in the DSC scans for these specimens.

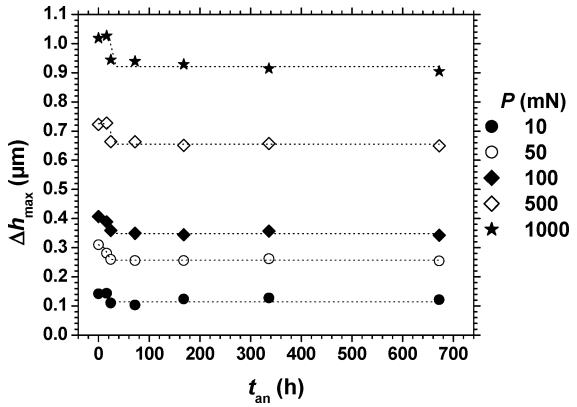

Figure 14. Shift in the maximum indentation depth vs the annealing time after indentation with five different loads.

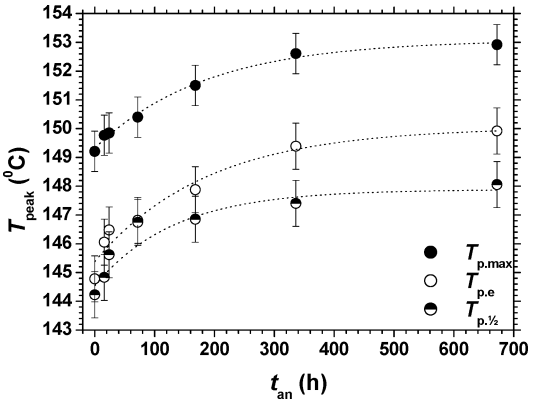

Figure 15. Changes in the $T_{p,e}$, $T_{p,1/2}$, and $T_{p,max}$ temperatures of polycarbonate upon annealing at 125 °C for 1 month.

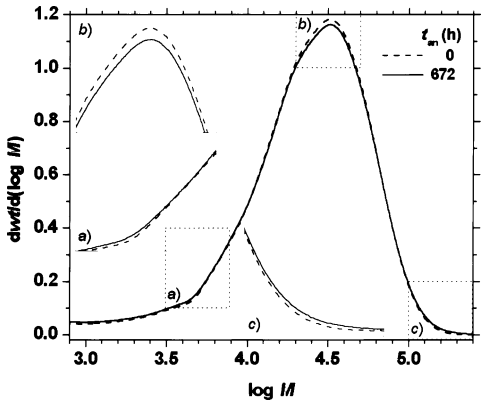

Figure 16. Molecular weight distribution for two specimens from set B, i.e., specimen B1, which was rejuvenated and not annealed, and specimen B7, which was annealed for 672 h at 125 °C after the rejuvenation. The incorporations are the three enlarged MWD fragments.

d. GPC Analysis. The gel permeation chromatography experiments (Figure 16) showed that molecular weight distribution of all polycarbonate samples analyzed was in good agreement with the average molecular weight claimed by the producer, which is approximately 30 000 (4.48 in a log scale).

The GPC experiments, which were performed on set B (Table 1), revealed a small gradual broadening of the MWD with an increase in the annealing time. This gradual change, which was best observable at a molecular weight of about 30 000, appeared to be reproducible (Figure 16).

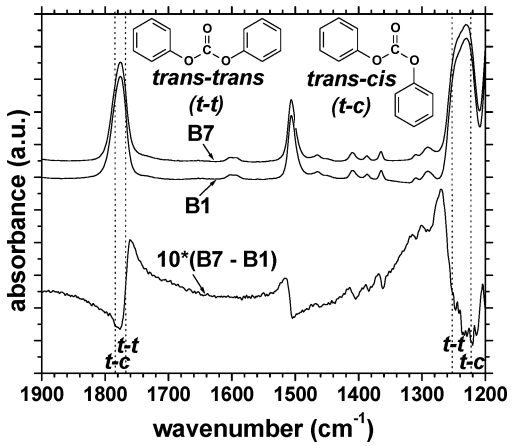

Figure 17. Fragments of the FTIR transmission spectra of the specimen annealed for 672 h at 125 °C (specimen B7) and the nonannealed one (specimen B1) and their difference spectrum, i.e., 10 (B7−B1), showing the evidence of the changes in the trans−trans and trans−cis conformational populations after annealing. The incorporations are the chemical structures of the trans−trans (*t*−*t*) and trans−cis (*t*−*c*) conformers of diphenyl carbonate.

e. ATR-IR and FTIR Transmission Analyses. The ATR-IR spectra obtained for the specimens forming set B (Table 1) are shown in Figure 5 for different annealing times. As one can see from these spectra, no clearly noticeable changes upon annealing took place, indicating that the polycarbonate was to a large extent chemically stable. However, for observing any minor changes such as conformational ones, a more detailed analysis is needed. A thorough analysis of the ATR-IR difference spectra pointed to an increase in the trans−trans conformational population at 1775 and 1235 cm^{-1} IR regions in the annealed specimens (specimens B2−B7 in Table 1) as compared to the nonannealed one (specimen B1). Unfortunately, no smooth increase in ratio between the trans−trans and trans−cis conformational populations upon increasing the annealing time was found. The fact that ATR-IR spectra are sensitive to the pressure with which the specimen is applied to the germanium crystal in the ATR accessory[7] can explain the absence of a proper correlation.

A comparison between the mean FTIR transmission spectra revealed clear changes between the conformational populations at two IR regions. These are the same IR regions at which the conformational interchange in the ATR-IR spectra was observed. The comparison of the doublets corresponding to the carbonyl band at ∼1775 cm^{-1} and the C−O−C antisymmetric vibration at ∼1235 cm^{-1} revealed that the population of trans−trans conformers is higher for the specimens annealed at 125 °C for 672 and 336 h (specimens B7 and B6) than for the nonannealed one (specimen B1). The trend observed in the difference spectra (Figure 17) is very similar to those reported in the literature for these conformational changes.[21] The maximum of the peak, which corresponds to the trans−trans conformational contribution at 1785 cm^{-1} of the carbonyl band, perfectly matched the maximum observed by Heymans[7] for the same region. Note that the locations of the peaks in the difference spectrum, which correspond to trans−trans and trans−cis conformational contributions, appeared with minor shifts as compared to the locations indicated originally in the literature (dotted lines in Figure 17).[22]

A comparison of the third IR region analyzed, corresponding to C−C aromatic in-plane stretching, appeared to be controversial, since no alteration in the trans−trans and trans−cis conformational populations was found (Figure 17). This observation is similar to the findings by Lu et al.[21] It is believed, therefore, that this band is the least sensitive to the conformational interchange among the three IR ranges analyzed.

f. Discussion of Physical Aging at Elevated Temperature. A comparison of the changes observed for E, H, and Δh_{max} and changes in the endothermic peak for similar annealing times showed that there is no linear correlation between the mechanical and the enthalpy changes found (cf. Figures 12, 14, and 15). The changes in E and H appear to be small in magnitude and dependent on penetration depth of the indenter. In the case of the small displacements, the changes in E and H took place predominantly at the first 24 h of annealing. For the endothermic peak, however, in the same time frame, the changes were minor. Upon further annealing, a more significant increase in $T_{p,e}$, $T_{p,1/2}$, and $T_{p,max}$ was observed. These observations are in good agreement with experimental results earlier reported by Hutchinson et al.,[6] who used the same polycarbonate grade and annealing procedure. The results obtained by Hutchinson et al. after their enthalpy relaxation experiments will be compared with ours results in more detail below.

Typically, changes observed in the mechanical properties upon annealing are attributed to densification of the material. However, a more focused look at the literature data concerning the decrease in free volume as a function of annealing time at constant temperatures discloses some contradictions.

On one hand, using electron spin resonance spectroscopy and dilatometry, Bartos et al.[19] showed that polycarbonate densifies gradually with higher densification rates for higher annealing temperature. Furthermore, somewhat different results were presented by Davis and Pethrick.[18] After using positron annihilation lifetime spectroscopy (PALS) and Doppler broadening spectroscopy, they reported that the orthopositronium (o-Ps) intensity, representing the free volume concentration, decreases upon annealing at different temperatures with a major decrease occurring over first 10−200 h of annealing time. They attributed these changes to structural relaxation of the polycarbonate.

On the other hand, Hill et al.[5] and Higuchi et al.,[9] who used PALS at annealing temperatures of 120 and 135 °C, respectively, concluded that the mean free volume cavity size and free volume concentration remained constant during annealing and that the changes in properties of polycarbonate were related to a decrease in the quasi-equilibrium free volume state of the material upon cooling[5] with an increase in stress relaxation time with decreasing cooling rate.[9]

A comparison of the above-presented literature data with our investigation showed that the results presented for indentation loads of 10, 50, and 100 mN in Figure 12 are in reasonable agreement with Davis and Pethrick's work. The comparison between E after indentation with 10 and 100 mN and the curve fitted to the o-Ps intensity vs t_{an} experimental results for annealing temperature of 80 °C[18] is shown in Figure 18. The major increase in E occurred in a similar time frame as polycarbonate densified according to the o-Ps intensity data. Moreover, on the basis of the experimental results given in Figure

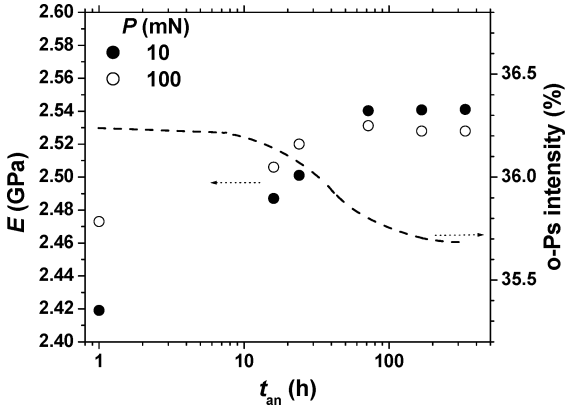

Figure 18. Comparison of the elastic modulus data after indentation with 10 and 100 mN on the specimens annealed at 125 °C with the results provided by Davis and Pethrick[18] concerning changes in the o-Ps intensity upon annealing at 80 °C for similar annealing time. Note that the values for the elastic modulus at $t_{an} = 0$ were shifted to $t_{an} = 1$ for an easier representation of annealing time on a logarithmic scale.

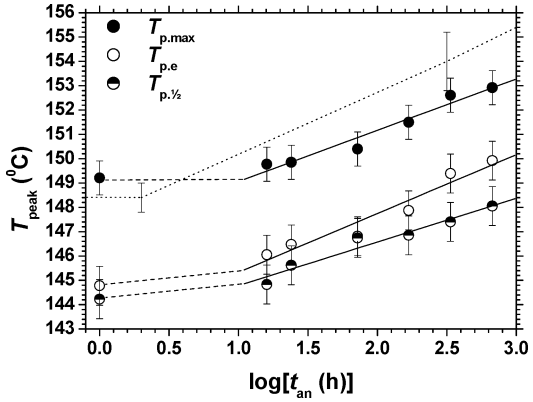

Figure 19. Changes in the $T_{p,e}$, $T_{p,1/2}$, and $T_{p,max}$ temperatures of polycarbonate upon annealing at 125 °C after our DSC experiments (dots) and after the alternating DSC experiments performed by Hutchinson et al.[6] (dotted lines corresponding to $T_{p,max}$). Note that the values for the temperatures at $t_{an} = 0$ were shifted to $t_{an} = 1$ for an easier representation of annealing time on a logarithmic scale.

12, one can assume that, in the case of indentation with loads above 1000 mN when "deeper layers" of polycarbonate are examined, no change in E and H upon annealing might be expected. Such a mechanical behavior of the bulk of polycarbonate would be in line with the PALS results, where no changes in free volume in polycarbonate upon annealing were revealed.[5,9]

Furthermore, knowing that PALS experimental data are dependent on the positron incident energy, which defines the mean implantation depth,[36] it is conceivable that the results provided by Davis and Pethrick represent the mean free volume changes in the layers closer to the polycarbonate surface than those after Hill et al.[5] and Higuchi et al.[9] Moreover, as was observed in the case of polystyrene,[36] a free volume and hole distribution closer to the surface might be different from that in the bulk of a polymer, Thus, because of the inhomogeneous free volume distribution, physical aging at an elevated temperature, as described by free volume changes, seems to occur with a gradient-like trend from the surface into the bulk. This may be the reason why some variations in elastic modulus and hardness values in relation to penetration depth were observed in the present work.

The experimental results highlighting the changes in creep behavior of polycarbonate upon annealing (Figures 13 and 14) appear to be in line with the results obtained for the elastic modulus and hardness. Similar to E and H with loads $\leq$ 100 mN, a change in creep behavior occurred over first hours of annealing (see section 2.2 for details on creep experiments).

As one can expect, changes in free volume during annealing can be caused by various phenomena, such as gas release, changes in local interchain packing density, alteration of the MWD, etc. The analytical data obtained by means of gel permeation chromatography showed that some broadening of the MWD during annealing occurred. It is believed that small amounts of short linear and/or cyclic polycarbonate oligomers, which are always present in the material, react further during annealing, and this is the main reason why the broadening of the MWD of polycarbonate took place during annealing.

Furthermore, ATR-IR and FTIR transmission spectroscopy showed that some trans−cis into trans−trans conformational interchange also occurred upon annealing (Figure 17), confirming thus the earlier reported observations claiming that trans−trans conformers, which allow closer local packing of the polymer chains, are more energetically favorable than trans−cis conformers.[7,21,22] This observation therefore indicates that a local decrease in free volume of polycarbonate occurred in fact during annealing.

A number of authors reported already that the endothermic peak shifts toward higher temperatures and increases in magnitude upon annealing.[6,14,16,17] For example, Orreindy and Rincon[14] observed an increase in T_g of 2.5 °C after annealing for 5 h at 130 °C. The shift of the endothermic peak observed during our DSC experiments on polycarbonate (Figure 15) confirmed this observation. The increase in $T_{p,max}$ found for our specimens matched particularly well with the work performed by Hutchinson et al.,[6] who used the similar polycarbonate grade and annealing temperature of 125 °C. Our experimental results (dots) in combination with those after Hutchinson et al. (dotted lines)[6] are presented in Figure 19.

One may consider that the enthalpy changes occurring during annealing are typically attributed to densification of polymers, and the present work provided an indirect proof for alterations in free volume and confirmed the shift of the endothermic peak toward higher temperatures during the annealing of polycarbonate. However, it is still unclear whether these changes are linked and that volumetric changes play a main role in the enthalpy changes. Furthermore, there are no reports in the literature showing changes in DSC scans, which would exceed the fault of DSC measurements, during aging of polycarbonate at room temperature. Moreover, no changes in $T_{p,e}$ and $T_{p,1/2}$ upon aging at room temperature were observed in the present work, although a significant decrease in free volume after approximately of 4−6 months of aging was found.[15,35] Remembering that the definition of enthalpy at constant pressure is $\Delta H_p = \Delta U + P\Delta V$, where H_p stands for enthalpy at constant pressure, U for internal energy, P for pressure, and V for volume, it appears that internal energy may also play a significant or dominant role in enthalpy changes. The partial conformational interchange between trans−cis and trans−trans conformers, which was observed in the present work as well as reported by other authors, appeared to be in line with

this idea, since closer local packing of the polymer chains, which is allowed by trans−trans conformers, is very likely to enhance van der Waals bonding and/or electrostatic interactions along the polymeric chains.[37] Furthermore, the broadening of the MWD is an oblique proof for changes in the internal energy of polycarbonate as well. It is unclear at this moment, however, whether the changes occurring in the internal energy due to closer local interchain packing and due to changes of the MWD are complementary or counteractive.

Furthermore, Greer and Wilkes showed in their work[17] that the internal energy plays an undoubtedly important role in the physical aging process. They found an apparent reversal of physical aging through enthalpy relaxation analysis after exposing polycarbonate to electron beam irradiation. During this deaging at $T < T_g$ there was no change in density observed. Furthermore, they found a strong correlation between scission of polycarbonate chains and the deaging process, indicating thus that the number of end groups plays a significant role in the internal energy state of glassy polymers.

Thus, in the case of annealing of polycarbonate, a decrease in the internal energy may take place even without significant change in free volume. This increase might possibly be caused by a postpolymerization process through covalent bonding of the existing chains and via enhancement in van der Waals bonding and/or electrostatic interactions along the polymeric chains at elevated temperatures. Another chemical modification, such as cross-linking, may also take place. The changes in the internal energy associated with the broadening of the MWD, and enhancement in van der Waals bonding and/or electrostatic interactions can explain the evident enthalpy changes upon annealing and the absence of such in polycarbonate aged at room temperature. Note also that, if the idea of inhomogeneous free volume distribution in the polymer is excluded, then, on the other hand, closer local interchain packing needed for enhancement in van der Waals bonding and/or electrostatic interactions appears to be contradictory to volumetric steadiness observable upon annealing by some authors.[5,9,17]

g. Final Remarks on Aging at Elevated Temperature. From the above presented discussion, it seems plausible that a number of competitive physicochemical phenomena take place in polycarbonate during annealing. First, trans−cis to trans−trans conformational transitions, which allow closer local interchain packing of the polymeric chains, enhance van der Waals bonding and/or electrostatic interactions along the polymeric chains. This, subsequently, decreases the internal energy of the polymer and causes changes in the enthalpy of polycarbonate. Second, possible postpolymerization, scission, and/or cross-linking processes, happening at similar annealing conditions and time, cause broadening of the MWD of the polymer and subsequently alter the free volume distribution in the polymer as well as its internal energy. Third, other phenomena may cause volumetric changes too, for instance, gas release at elevated temperatures from the embedded cavities. Finally, it is believed that all these phenomena occur in the polymer having an inhomogeneous free volume distribution from the surface to the bulk, different molecular mobility, and therefore presumably different predominance of the competitive events in various geometrical locations within the polymer.

4. Conclusions

The load and depth sensing indentation technique was successfully used in order to assess the changes occurring in elastic modulus, hardness, and creep of polycarbonate of bisphenol A during aging at room and elevated temperatures. In combination with DSC measurements, an obvious difference between aging at different temperatures in terms of mechanical properties and a shift of the endothermic peak was observed.

The stepwise increase in the elastic modulus and hardness of polycarbonate was observed after approximately the same aging time as the peculiar transition in the densification behavior of polycarbonate occurred (Figures 10 and 11). Furthermore, this stepwise change appeared to be identical in magnitude to the change observed for the storage modulus at room temperature after a minor increase in orientation of polycarbonate chains.[3] This suggests that the observed stepwise increase in the elastic modulus is linked to the densification of polycarbonate due to changes in orientations of the polymeric chains.

It is believed that free volume has an inhomogeneous, presumably gradient-like, distribution in polycarbonate, with a larger concentration and/or size of the cavities closer to the surface than in the bulk. As ramification of that, the densification of polycarbonate upon annealing occurs inhomogeneously, with a more significant decrease in free volume closer to the surface and a smaller or no decrease in the bulk. This is reflected in the changes of the elastic modulus and hardness values corresponding to different penetration depths.

We found no linear correlation between the changes in the mechanical properties and the enthalpy changes occurring during annealing. This observation is in good agreement with findings of Hutchinson et al.[6] The changes in the mechanical properties and the enthalpy changes are believed to be mainly associated with different phenomena causing them. The changes in the elastic modulus, hardness, and creep may be largely attributed to the volumetric changes occurring upon annealing, whereas the shift of the endothermic peak and its increase in magnitude may be explained by variations in the internal energy of polycarbonate.

The IR and GPC analyses provided evidence of conformational interchange and alterations in molecular weight distribution during annealing, respectively. Both these phenomena lead to changes in free volume and internal energy of the polymer. The variations found, however, could not elucidate the reason why major changes in mechanical properties and in the location/magnitude of the endothermic peak occurred at different annealing times.

Acknowledgment. The authors are grateful to Dr. J. Malzbender (Institute for Materials and Processes in Energy Systems, Jülich, Germany) and Eng. M. H. C. Janssen (Domestic Mechanical Workshop Department, Eindhoven University of Technology (TU/e), Eindhoven, The Netherlands) for useful discussions concerning load and depth sensing indentation measurements and working principles of the DSI apparatus, respectively. We also thank Mr. H. A. M. van der Palen (Laboratory of Solid State and Materials Chemistry, TU/e, Eindhoven, The Netherlands) for help with specimen preparation, Mr. W. J. Kingma (Laboratory of Polymer Chemistry, TU/e, Eindhoven, The Netherlands) for GPC analyses, and Dr. R. D. van de Grampel (G.E. Plastics,

Bergen op Zoom, The Netherlands) for valuable information concerning some properties of polycarbonate. We are also grateful to Dr. G. de Wit (G.E. Plastics, Bergen op Zoom, The Netherlands) for his comments on the manuscript and to Mr. M. Romanelli for checking English grammar and punctuation. Finally, the authors are thankful to IOP (The Netherlands) for the financial support.

References and Notes

(1) Shnell, H. *Chemistry and Physics of Polycarbonates*; Wiley-Interscience: New York, 1964.
(2) LeGrand, D. G.; Bendler, J. T. *Handbook of Polycarbonate Science and Technology*; Marcel Dekker: New York, 2000.
(3) Shelby, M. D.; Hill, A. J.; Burgar, M. I.; Wilkes, G. L. *J. Polym. Sci., Polym. Phys. Ed.* **2001**, *39*, 32−46.
(4) Li, X.; Hristov, A.; Yee, A. F.; Gidley, D. W. *Polymer* **1995**, *36*, 759−765.
(5) Hill, A. J.; Heater, K. J.; Agrawal, C. M. *J. Polym. Sci., Polym. Phys. Ed.* **1990**, *28*, 387−405.
(6) Hutchinson, J. M.; Smith, S.; Horne, B.; Gourlay, G. M. *Macromolecules* **1999**, *32*, 5046−5061.
(7) Heymans, N. *Polymer* **1997**, *38*, 3435−3440.
(8) Shelby, M. D.; Wilkes, G. L. *Polymer* **1998**, *39*, 6767−6779.
(9) Higuchi, H.; Yu, Z.; Jamieson, A. M.; Simha, R.; Mcgervey, J. D. *J. Polym. Sci., Polym. Phys. Ed.* **1995**, *33*, 2295−2305.
(10) Brauwens-Crowet, C. *J. Mater. Sci.* **1999**, *34*, 1701−1709.
(11) Guest, M. J.; van Daele, R. *J. Appl. Polym. Sci.* **1995**, *55*, 1417−1429.
(12) Bendler, J. T. *Comput. Theor. Polym. Sci.* **1998**, *8*, 83−92.
(13) Othmezouri-Decerf, J. *J. Mater. Sci.* **1999**, *34*, 2351−2359.
(14) Orreindy, S.; Rincón, G. A. *J. Appl. Polym. Sci.* **1999**, *74*, 1646−1648.
(15) Robertson, G. C.; Wilkes, G. L. *Macromolecules* **2000**, *33*, 3954−3955.
(16) Hutchinson, J. M.; Tong, A. B.; Jiang, Z. *Thermochim. Acta* **1999**, *335*, 27−42.
(17) Greer, R. W.; Wilkes, G. L. *Polymer* **1998**, *18*, 4205−4210.
(18) Davis, W. J.; Pethrick, R. A. *Eur. Polym. J.* **1998**, *34*, 1747−1754.
(19) Bartos, J.; Müller, J.; Wendorff, J. H. *Polymer* **1990**, *31*, 1678−1684.
(20) Lee, S.-N.; Stolarski, V.; Letton, A.; Laane, J. *J. Mol. Struct.* **2000**, *521*, 19−23.
(21) Lu, J.; Wang, Y.; Shen, D. *Polym. J.* **2000**, *32*, 610−615.
(22) Schmidt, P.; Dybal, J.; Turska, E.; Kulczycki, A. *Polymer* **1991**, *32*, 1862−1866.
(23) Jones, A. A. *Macromolecules* **1985**, *18*, 902−906.
(24) Dybal, J.; Schmidt, P.; Baldrian, J.; Kratochvíl, J. *Macromolecules* **1998**, *31*, 6611−6619.
(25) Oliver, W. C.; Pharr, G. M. *J. Mater. Res.* **1992**, *7*, 1564−583.
(26) Ashcroft, I. A.; Spinks, G. M. *J. Mater. Res.* **1996**, *11*, 529−536.
(27) Malzbender, J.; de With, G. *J. Non-Cryst. Solids* **2000**, *265*, 51−60.
(28) Pharr, G. M. *Mater. Sci. Eng. A* **1998**, *253*, 151−159.
(29) Simmons, G.; Wang, H. *Single-Crystal Elastic Constants and Calculated Aggregated Properties*: *A Handbook*; MIT Press: Cambridge, MA, 1971.
(30) Porter, D. *Group Interaction Modeling of Polymeric Properties*; Marcel Dekker: New York, 1995.
(31) Bolshakov, A.; Pharr, G. M. *J. Mater. Res.* **1998**, *13*, 1049−1058.
(32) Höhne, G.; Hemminger, W.; Flammersheim, H.-J. *Differential Scanning Calorimetry*: *An Introduction for Practitioners*; Springer-Verlag Berlin, 1996.
(33) Young, R. J.; Lovell, P. A. *Introduction to Polymers*, 2nd ed.; Chapman & Hall: London, 1991.
(34) Boersma, A.; Soloukhin, V. A.; Brokken-Zijp, J. C. M.; de With, G., submitted to *J. Polym. Sci., Polym. Phys. Ed.*
(35) Wimberger-Friedl, R.; de Bruin, J. G. *Macromolecules* **1996**, *29*, 4992−4997.
(36) Cao, H.; Yuan, J.-P.; Zhang, R.; Sunder, C. S.; Jean, Y. C.; Suzuki, R.; Ohdaira, T.; Nielsen, B. *Appl. Surf. Sci.* **1999**, *149*, 116−124.
(37) Pozuelo, J.; Baselga, J. *Polymer* **2002**, *43*, 6049−6055.

MA0342980